Conformational Changes of the in Situ Nuclear Pore Complex

Hongwei Wang and David E. Clapham
Howard Hughes Medical Institute, Harvard Medical School, Boston, Massachusetts 02115 USA

ABSTRACT By bridging the double membrane separating the cell nucleus and cytoplasm, nuclear pore complexes (NPCs) are crucial pathways for the exchange of ions, proteins, and RNA between these two cellular compartments. A structure in the central lumen of the NPC, called the nuclear transport protein, central granule, or nuclear plug, appeared to gate diffusion of intermediate-sized molecules (10–40 kDa) across the nuclear membranes. Visualization of the NPC required drying and fixation of the specimen for electron and atomic force microscopy (AFM), a requirement that has raised doubts about the physiological relevance of the observation. Here we present AFM images of the outer nuclear membranes and NPCs of *Xenopus laevis* oocytes under more physiological conditions. Measured under a variety of Ca^{2+} depletion conditions, the central granule appeared to occupy and occlude the lumen of the pore in >80% of NPCs compared to <10% in controls. In a few instances images were obtained of the same NPCs as the solution was changed from control saline to store depletion conditions, and finally to store repletion conditions. We conclude that the central lumen of the nuclear pore complex undergoes a conformational change in response to depletion of nuclear cisternal Ca^{2+} levels.

INTRODUCTION

The nuclear envelope encloses the genetic material of a eukaryotic cell with two lipid bilayer membranes and associated nuclear lamina. A nuclear pore complex (NPC) spans the inner and outer nuclear membranes and provides the route for nuclear traffic (for review see Forbes, 1992; Hanover, 1992; Pante and Aebi, 1994; Goldberg and Allen, 1995; Perez-Terzic et al., 1997; Allen et al., 1998; Mattaj and Englmeier, 1998). Extensively investigated by electron microscopy, the NPC is a macromolecule of ≅124,000 kDa comprised of 100–200 different polypeptides that form a tripartite structure consisting of a spoke complex, and cylindrical cytoplasmic and nuclear rings (Hinshaw et al., 1992; Akey and Radermacher, 1993). The number of NPCs present in the nuclear envelope correlates with metabolic activity and may vary from 1 pore/μm^2 to 50 pores/μm^2 (Gerace and Burke, 1988).

Seen from the cytoplasmic surface, the NPC has eightfold symmetry surrounding a central lumen. A central granule occupies the NPC lumen but its role is poorly understood. There are three main hypotheses for the central granule's role in the NPC (cf. Akey, 1990; Jarnik and Aebi, 1991). The first is that the central granule represents protein components of the NPC that participate in the active transport of molecules across the nuclear envelope. The second hypothesis is that the central granule represents cargo caught in transit across the NPC. Finally, the central granule might be an artifact caused by, for example, the nuclear basket collapsing into the NPC lumen during fixation.

Received for publication 11 January 1999 and in final form 22 April 1999.
Address reprint requests to David E. Clapham, M.D., Ph.D., Investigator, Howard Hughes Medical Institute, Professor of Neurobiology, Professor of Pediatrics, Children's Hospital, Harvard Medical School, 1309 Enders, 320 Longwood Avenue, Boston, MA 02115. Tel.: 617-355-6163; Fax: 617-355-3692; E-mail: clapham@rascal.med.harvard.edu.
© 1999 by the Biophysical Society
0006-3495/99/07/241/07 $2.00

While the transport of transcription factors and nuclear localization signal (NLS)-containing proteins into the nucleus has been extensively studied, little is known of the molecular mechanisms that regulate passive diffusion. Small molecules lacking an NLS (<~60 kDa) diffuse passively across the NPC and transit the nuclear boundary at rates that suggest that their size, not their structure, limits their entry and exit (Gerace and Burke, 1988). Several findings suggest that nuclear pore permeability can also be regulated. Passive diffusion can be decreased when an antibody raised against the lumenal domain of the gp210 nuclear protein is expressed in the endoplasmic reticulum (Greber et al., 1990; Greber and Gerace, 1992). Diffusion of smaller molecules was decreased when ER Ca^{2+} was released by a specific ionophore (Greber and Gerace, 1995). We found that Ca^{2+} depletion from the ER (rather than a rise in cytoplasmic [Ca^{2+}]) was required to block the passive diffusion of intermediate-sized molecules. When Ca^{2+} stores were depleted by IP_3 application to nuclei and nuclear ghosts, all nuclei were observed to exclude Calcium Green-dextran (10-kDa) from the nucleoplasm (Stehno-Bittel et al., 1995b). The effect of IP_3 was specific since related inositol polyphosphates that did not release Ca^{2+} failed to block diffusion of the 10-kDa molecule into the nucleoplasm. The blockade of intermediate-sized molecules was reversed by replenishing the intracisternal [Ca^{2+}] (e.g., through addition of Ca^{2+} and ATP to the bath). Exclusion of the 10-kDa dye was not dependent on nucleoplasmic binding since the same effects were observed in nuclear ghosts where the nuclear matrix was absent. Smaller molecules (500-Da Lucifer Yellow) and ions (Mn^{2+}) diffused freely into the nuclei even when cisternal Ca^{2+} was depleted (Stehno-Bittel et al., 1995b).

In previous work we tested whether the regulation of intermediate-sized molecule transit across the nuclear envelope could be related to conformational changes in the NPC. Field emission scanning electron microscopy (FESEM),

transmission electron microscopy (TEM), and atomic force microscopy (AFM) were employed to image the NPC under various conditions (Perez-Terzic et al., 1996; for AFM imaging of NPCs see also Folprecht et al., 1996 and Rakowska et al., 1998). With full nuclear Ca^{2+} stores, the central granule was recessed as visualized by FESEM and AFM of fixed specimens. Depletion of nuclear Ca^{2+} stores resulted in an apparent upward shift of the granule to a level even with the outer rim of the NPC. Furthermore, the internal diameter within the centrally tapered region of the NPC declined by half after Ca^{2+} store depletion. These results supported the hypothesis that the filling state of the nuclear Ca^{2+} store governs conformational changes in the nuclear pore complex. The conformational changes might gate transit of passively diffusing intermediate and small-sized molecules. A persistent worry has been that the fixation conditions needed to visualize these changes induce artifactual changes. As reported here, we used AFM to examine the conformational change of the NPCs on the unfixed nuclear envelope under more physiological conditions. Using continuous AFM measurements under physiologic saline solution we again found that the NPC complex central granule shifted by ~10 nm in the cytoplasmic direction and the NPC lumen narrowed upon Ca^{2+} store depletion.

MATERIALS AND METHODS

Preparation of the nuclear envelope

Adult female *Xenopus laevis* toads were anesthetized and their ovaries surgically removed. The oocyte coating was digested with collagenase in a solution containing (in mM): 82 NaCl, 20 $MgCl_2$, 1 KCl, 5 HEPES, pH 7.6. The mature oocytes were selected and placed in ND96 solution containing (in mM): 96 NaCl, 2 KCl, 1.8 $CaCl_2$, 5 HEPES, pH 7.6. Oocytes were dissected manually along their equator using two sharp forceps. The nuclei were isolated and transferred to the mock intracellular buffer (MIB) containing (in mM): 90 KCl, 10 NaCl, 2 $MgCl_2$, 0.75 $CaCl_2$, 1.1 EGTA (free Ca^{2+} ~200 nM), 10 HEPES, pH 7.32. After a 10-min incubation period, the intact nuclei were moved to a coverslip that had been coated overnight with poly-L-lysine (5 mg/ml) and kept at 4°C. Using sharp needles, the nuclear envelope was cleaved and spread manually on the coverslip with its nucleoplasmic side facing down. The NPCs were always kept in the same orientation (by a suction pipette) and placed one by one on the coverslip. The specimen was rinsed to remove chromatin and cytoplasm. The solution was withdrawn and replaced immediately (without drying) with fresh MIB. MIB was adjusted to low Ca^{2+} (~5–10 nM free Ca^{2+}), and in some experiments agents added or ionic conditions altered as described in the text.

Atomic force microscopy

A BioScope AFM (NanoScope IIIa, Digital Instruments, Santa Barbara, CA) was mounted on an inverted optical microscope. Standard V-shaped silicon nitride cantilevers and pyramidal tips were used. The tips were oxide-sharpened to an estimated diameter of 10–20 nm. Both contact and tapping modes were used in the experiments. In contact mode under fluid, the standard 200 μm-long V-shaped cantilever was used to image the specimen (spring constant 0.06 N/m). As soon as the tip engaged the specimen surface the force was minimized as estimated by prior force calibration. The set point (force value) was adjusted to slightly above the force curve. The specimen was scanned at 1–3 Hz, depending on the scan area. In tapping mode under fluid, the standard V-shaped 100 μm-long cantilever was employed for imaging (spring constant 0.38 N/m). In this case, the scan rate was adjusted to <0.5 Hz in order to prevent specimen damage. The advantage of tapping mode over contact mode was that in tapping mode the tip only transiently contacted the specimen surface, enabling the tip to be used for a longer time without contamination by biological material. Unfortunately, resolution was lower in tapping mode than contact mode. After the first image was recorded as a control, the tip's movement was stopped and the force calibrated. The medium was changed, equilibrated for ~10 min, and the tip returned to the surface for imaging as many times as shown for each experiment.

All measured values are given as the mean ± standard error of the mean (SEM). The temperature was 22 ± 2°C.

RESULTS

Sections of *Xenopus* oocyte nuclear membranes were removed directly from nuclei immersed in MIB and the cytoplasmic face imaged at room temperature using AFM (Fig. 1). The density of NPCs was 46 ± 11/um^2 (n = 4730 NPCs from 17 oocytes). Under physiological conditions, cytoplasmic free intracellular [Ca^{2+}] in oocytes varies from 50 to 200 nM (Lechleiter and Clapham, 1992). When imaged under these low [Ca^{2+}] conditions, close examination of NPCs revealed that there were two distinct conformations. In over 90% of NPCs, the eightfold symmetry of the individual NPC's cytoplasmic ring was visible and the central depression was not occluded (Fig. 2 *A*). In the remainder, a central granule apparently occluded the mouth of the pore (Fig. 2 *C*). Contact mode AFM images taken under these conditions showed that in 8 ± 2% of nuclei (n = 873 NPCs from six oocytes), the NPCs were occupied by the central granule. The central depression from nuclei in normal [Ca^{2+}] was 10 ± 1 nm (n = 12 profiles) in depth measured from the cytoplasmic surface (Fig. 2, *B* and *D*), compared to previous measurements in fixed oocytes of 12 ± 1 nm (Perez-Terzic et al., 1996). In the 8% of NPCs that were occluded under these conditions, the peak of the central granule was approximately level with the cytoplasmic ring (0.7 ± 0.2 nm below the rim; n = 15 profiles) similar to that previously measured fixed specimens (2 nm; Perez-Terzic et al., 1996). The average diameters of the inner and outer nuclear cytoplasmic rings were 46 ± 4 nm and 140 ± 6 nm as measured from the inner and outer rims of the NPCs, respectively, as projected in two dimensions (Table 1). This compares to 68 ± 2 and 149 ± 5 nm in fixed oocytes (Perez-Terzic et al., 1996).

To test the effect of nuclear cisternal Ca^{2+} depletion, nuclear envelopes were first prepared in normal Ca^{2+} (free [Ca^{2+}] ~200 nM) followed by a 10-min incubation in low [Ca^{2+}] medium (free [Ca^{2+}] ~10 nM). AFM imaging showed that the central granules now blocked most of the central depression of the NPCs, with 82 ± 4% of the pores occupied (n = 2854 NPCs from 11 oocytes). In a second method used to deplete nuclear cisternal Ca^{2+}, we incubated nuclei in 10 mM BAPTA [bis(2-aminophenoxy) ethane-*N*,*N*,*N*′,*N*′-tetraacetic acid; a rapid Ca^{2+} chelator] for 10 min. Imaged again in solution, 95 ± 4% (n = 1516 NPCs from six oocytes) of the NPCs were found to be occupied by

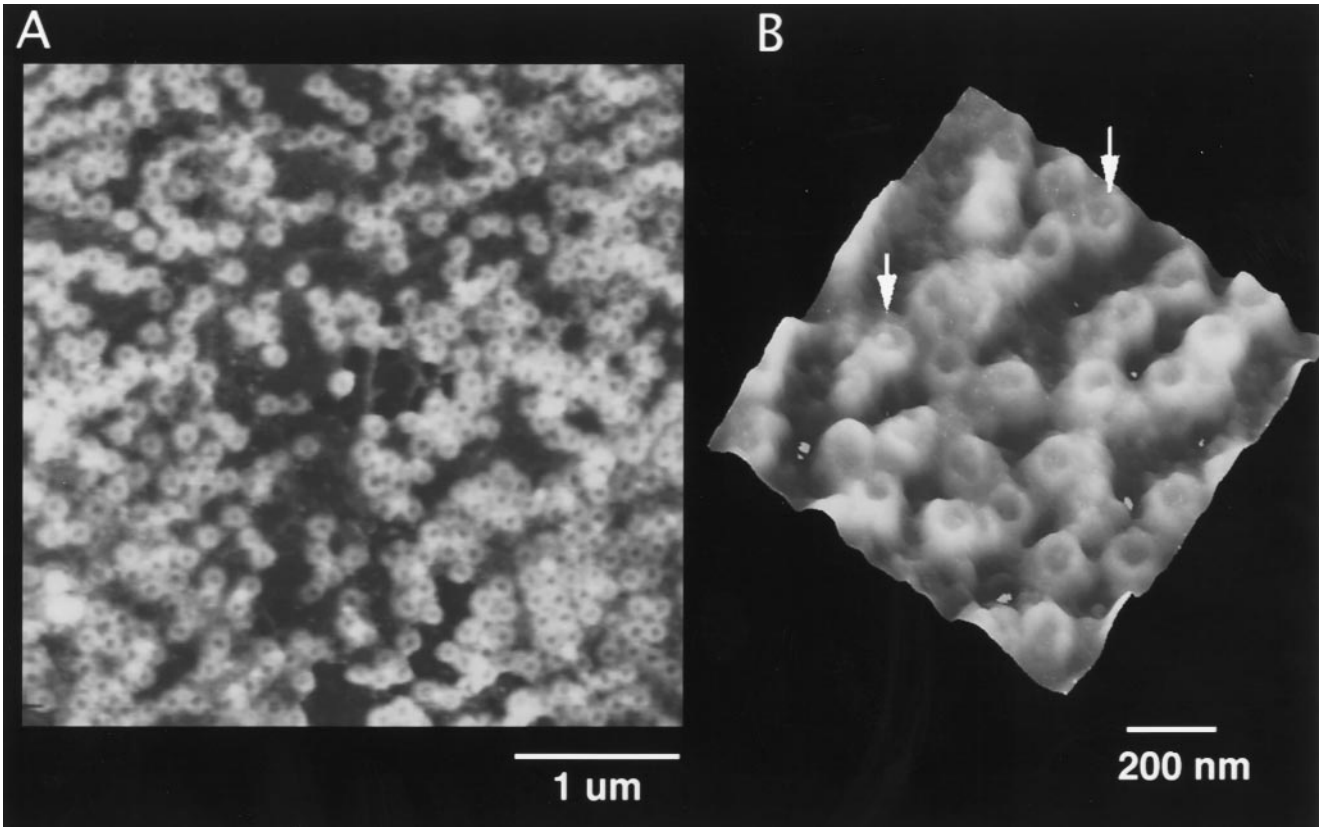

FIGURE 1 AFM images of *Xenopus* oocyte nuclear envelopes in MIB. (*A*) Top view of an ~16 μm^2 area showing the overall density and distribution of NPCs. (*B*) Three-dimensional representation of a scanned ~1 μm^2 area reveals that some of the NPC depressions are apparently occluded by the central granule (*white arrows*).

the central granule. Using a third method of store depletion, the Ca^{2+}-ATPase pump inhibitor, thapsigargin (1 μM), was added to the normal Ca^{2+} medium for 10 min before imaging. Again the majority of the NPCs imaged were found to be occupied by the central granule (90 ± 5%; n = 1801 NPCs from eight oocytes; Fig. 3). Conversely, if the nuclear envelopes were incubated in high Ca^{2+} medium (free Ca^{2+} = 500 nM), only 4 ± 1% (n = 3630 NPCs from eight

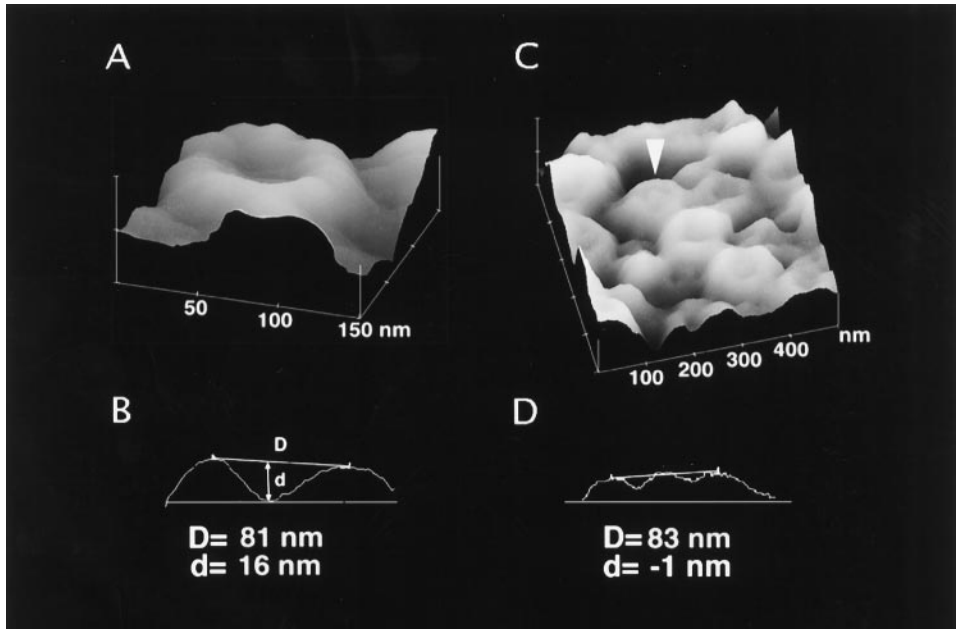

FIGURE 2 Three-dimensional images of *Xenopus* oocyte NPCs in MIB solution. (*A*) Image of one NPC incubated in normal (200 nM free [Ca^{2+}]) Ca^{2+}-containing medium. The AFM imaged NPC has the characteristic eightfold symmetry described in previous 2D electron microscopy. (*B*) Profile of the NPC showing an unusually recessed central depression (~16 nm in depth (*d*) as measured from the midpoint between the peaks of the NPC outer vestibule (D = 81 nm) to the lowest point between peaks). (*C*) Image of NPCs in which the central granule has shifted to occlude the central depression by Ca^{2+} depletion. (*D*) NPC profiles of (*C*) revealing occlusion of the central depression (d = −1 nm indicates that the central granule is 1 nm *above* the surrounding cytoplasmic rings).

TABLE 1 Nuclear pore complex diameter changes under AFM imaging in solution

Conditions	External NPC Diameter	Internal NPC Diameter	Depression
200 nM free calcium	140 ± 6 nm ($n = 52$)	46 ± 4 nm ($n = 52$)	9.7 ± 1.2 nm ($n = 52$)
1 μM IP_3	132 ± 7 nm ($p < 0.01$, $n = 52$)	33 ± 5 nm ($p < 0.01$, $n = 52$)	1.6 ± 0.2 nm ($n = 52$)
Ca^{2+} + ATP	142 ± 6 nm ($n = 52$)	47 ± 5 nm ($n = 52$)	8.4 ± 3.1 nm ($n = 52$)

oocytes) of NPCs contained the central granules. As shown in Fig. 4, the breakpoint in the control histogram (4 .5 nm) was chosen as the value defining whether the NPC was closed ($d < 4.5$ nm) or open ($d > 4.5$ nm).

Since small perturbations in flow result in movement of the preparation, most experimental trials were performed on independent specimens. However, we did succeed in obtaining a few experiments in which the solution was changed from control to store-depletion, and back again to store-repletion conditions, while imaging the same NPCs under AFM. In this experiment we also used the physiologic Ca^{2+} store agonist, inositol 1,4,5-trisphosphate (IP_3), to open the IP_3-gated Ca^{2+} channel and deplete the Ca^{2+} store. IP_3 receptors are abundant on the outer nuclear membrane (Mak and Foskett, 1994; Stehno-Bittel et al., 1995a). Thus IP_3 was previously used to deplete stores and block diffusion into intact nuclei (Stehno-Bittel et al., 1995b) and as a Ca^{2+}-depletion pretreatment in fixed specimens (Perez-Terzic et al., 1996). In the present experiments we first incubated the nuclei in normal Ca^{2+} medium and imaged the nuclear envelope surface (Fig. 5 *A*). The medium was then changed to a solution containing 1 μM IP_3 for 10 min and the same area imaged (Fig. 5 *B*). Occluded pore depressions increased from 16% in controls to 66% in Ca^{2+}-depleted conditions. Finally, the stores were repleted by incubation in 1 mM adenosine triphosphate (ATP 1 mM) plus high Ca^{2+} (free $[Ca^{2+}] = 500$ nM; see Perez-Terzic et al., 1996) and the sample incubated for 10 min before AFM imaging (Fig. 5 *C*). Ca^{2+} store repletion decreased the percentage of obscured lumens from 66% to 27%. During these exchanges, the nuclear envelope was never dry and the images were taken from the same patch of nuclear envelope. Although the image was slightly shifted by the solution changes, the same NPCs were imaged under all three conditions. These changes were comparable but less dramatic than averaged individual experiments in which the values were 8 ± 2% ($n = 873$ NPCs from six oocytes), 90 ± 3% ($n = 2831$ NPCs from 14 oocytes) and 19 ± 6% ($n = 1856$ NPCs from 10 oocytes) for control, IP_3-induced Ca^{2+} depletion, and Ca^{2+} repletion, respectively. Table 1 summarizes the changes in the inner and outer diameters of the NPC. In contrast to our previous findings under fixed conditions in which the inner diameter was halved from 68 to 34 nm, the NPC diameter imaged in MIB was decreased by 30%, from 47 to 33 nm.

DISCUSSION

Conclusions based on structural determination of protein conformations are usually qualified by the nonphysiologic conditions needed for most imaging techniques. For the NPC, this has given rise to uncertainties about the significance of the central granule, or nuclear transporter. The large size of the macromolecular NPC permits AFM imaging of the NPC complex in mock intracellular solutions and, in rare instances, even continuous imaging during solution changes. We have extended our previous observations that the nuclear pore complex undergoes conformational changes upon depletion of Ca^{2+} from the nuclear cisterna to these more physiological conditions. The experiments in MIB show that the NPC undergoes a reversible conformational change upon store depletion with an upward shift of the central granule by ~10 nm toward the cytoplasmic face,

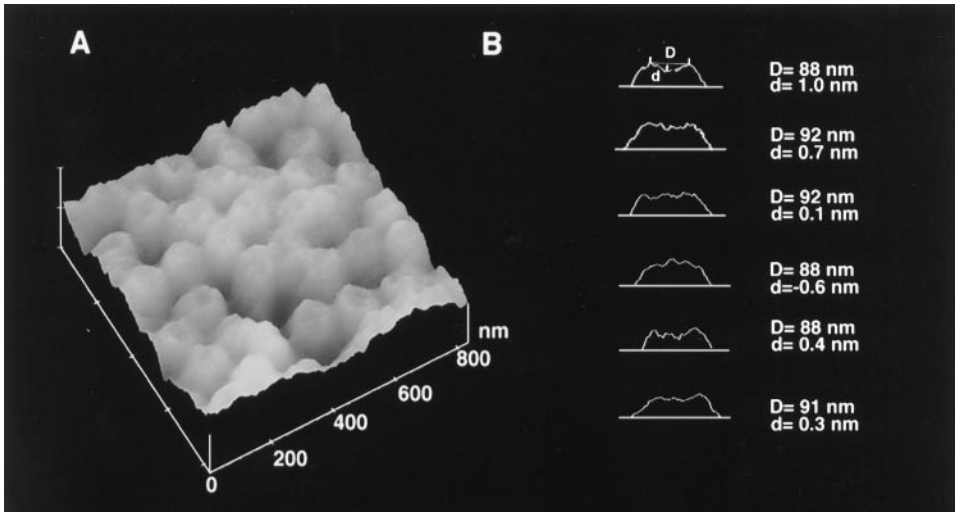

FIGURE 3 Images of NPCs in Ca^{2+}-depleted solutions. (*A*) Nuclei were incubated in the low Ca^{2+} (free Ca^{2+} ~5 nM) and imaged over an ~4 μm^2 area. (*B*) Sample profiles of Ca^{2+}-depleted NPCs showing the range of measurements. Distances *d* and *D* are the same as defined in Fig. 2.

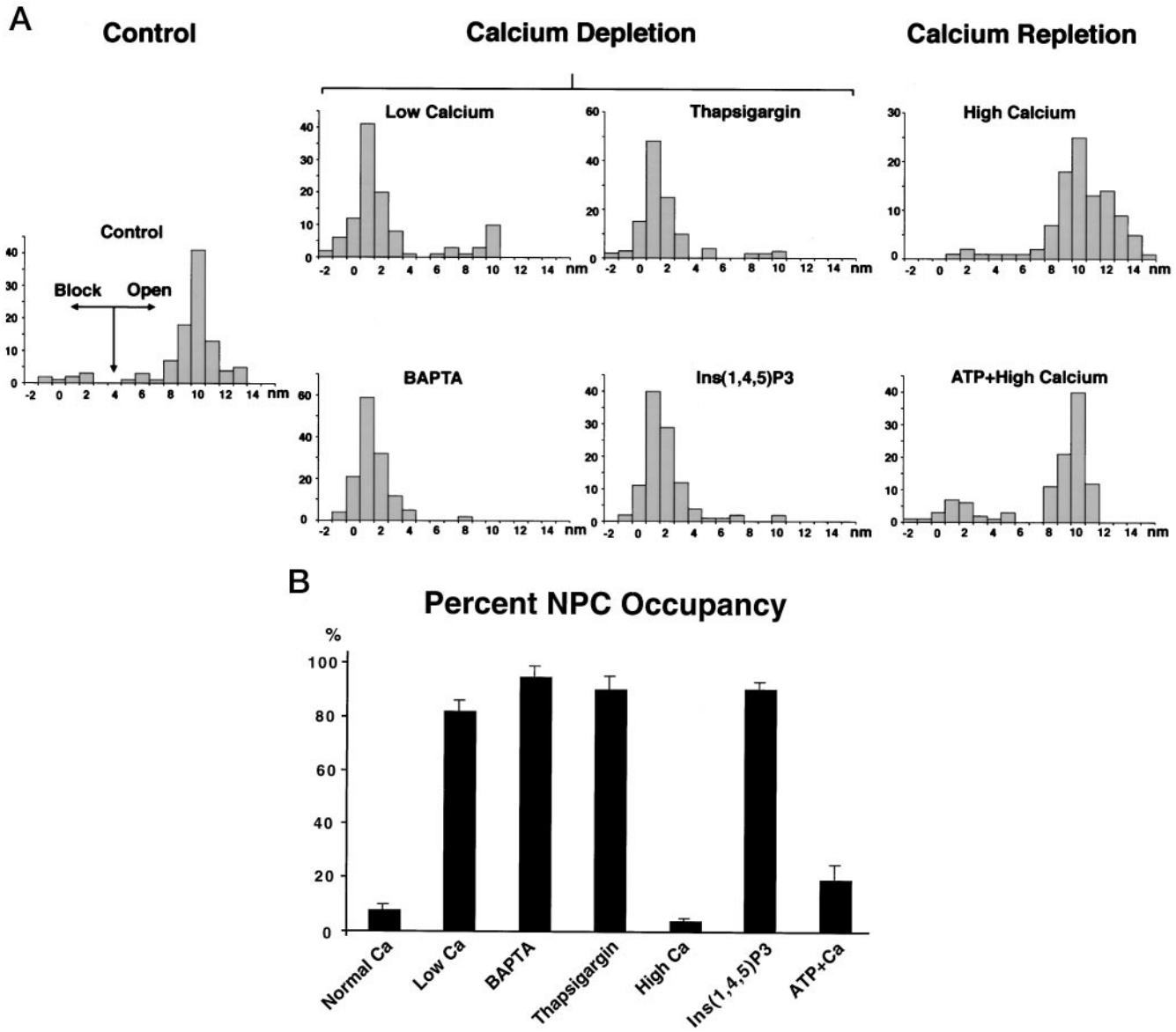

FIGURE 4 (*A*) Histograms of the depth (*d*) measured from the cytoplasmic ring to the top of the central granule (see Fig. 2). The *y* axis indicates the number of NPCs measured under each condition, while the depth (*d*) in nm is plotted on the *x* axis. The breakpoint in the control histogram (4 .5 nm) was chosen as the value defining whether the NPC was closed ($d \leq 4.5$ nm) or open ($d > 4.5$ nm). All Ca^{2+} store depletion conditions, such as incubation in 10 nM free [Ca^{2+}], 1 μM thapsigargin, 10 mM BAPTA, or 1 μM IP_3, resulted in movement of the central granule to the closed NPC position. Replenishing the Ca^{2+} store by incubation in 500 nM Ca^{2+} or 500 nM Ca^{2+} and 1 mM ATP resulted in the movement of the central granule back to its control (open) position. (*B*) Central granule occupancy of the central depression from nuclei under various Ca^{2+}-depletion conditions. The percentage increased from 8% ($\pm$2%, $n = 6$) in normal Ca^{2+} solution to 82% ($\pm$4%, $n = 11$) in low (10 nM) Ca^{2+}, 95% in 10 mM BAPTA ($\pm$4%, $n = 6$), and 90% in 1 μM thapsigargin-treated ($\pm$5%, $n = 8$) nuclei. After repletion of stores by incubation in high Ca^{2+}, the percent occupancy declined to 4% ($\pm$1%, $n = 8$). After depleting the Ca^{2+} store with Ins(1,4,5)P_3, the percent occupancy again increased to 90% ($\pm$3%, $n = 14$) followed by a decline to 19% ($\pm$6%, $n = 10$) after repletion in 1mM ATP and 500 nM [Ca^{2+}].

while undergoing a 30% decline in the inner pore diameter from 47 to 33 nm. This compares to a 12 nm upward shift of the central granule and a halving of the central lumen of the NPC from 68 nm to 34 nm as measured in fixed NPCs (Perez-Terzic et al., 1996).

Since the nuclear cisterna is continuous with the endoplasmic reticulum, it is not surprising that Ca^{2+} is released from this space by IP_3 receptor agonists or that Ca^{2+}ATPase pumps import Ca^{2+} to replete these stores. Work by Greber and Gerace (1995) suggested that Ca^{2+} release from nuclear stores resulted in block of free diffusion of lower molecular weight molecules. Our laboratory confirmed this finding for free diffusion (Stehno-Bittel et al., 1995b), but in contrast to Greber et al. (1997), not for actively transported molecules (Strübing and Clapham, 1999). Depletion of stores, rather than a rise in cytoplasmic Ca^{2+}, was the event that led to block of intermediate-weight molecular diffusion across nuclear membranes in intact

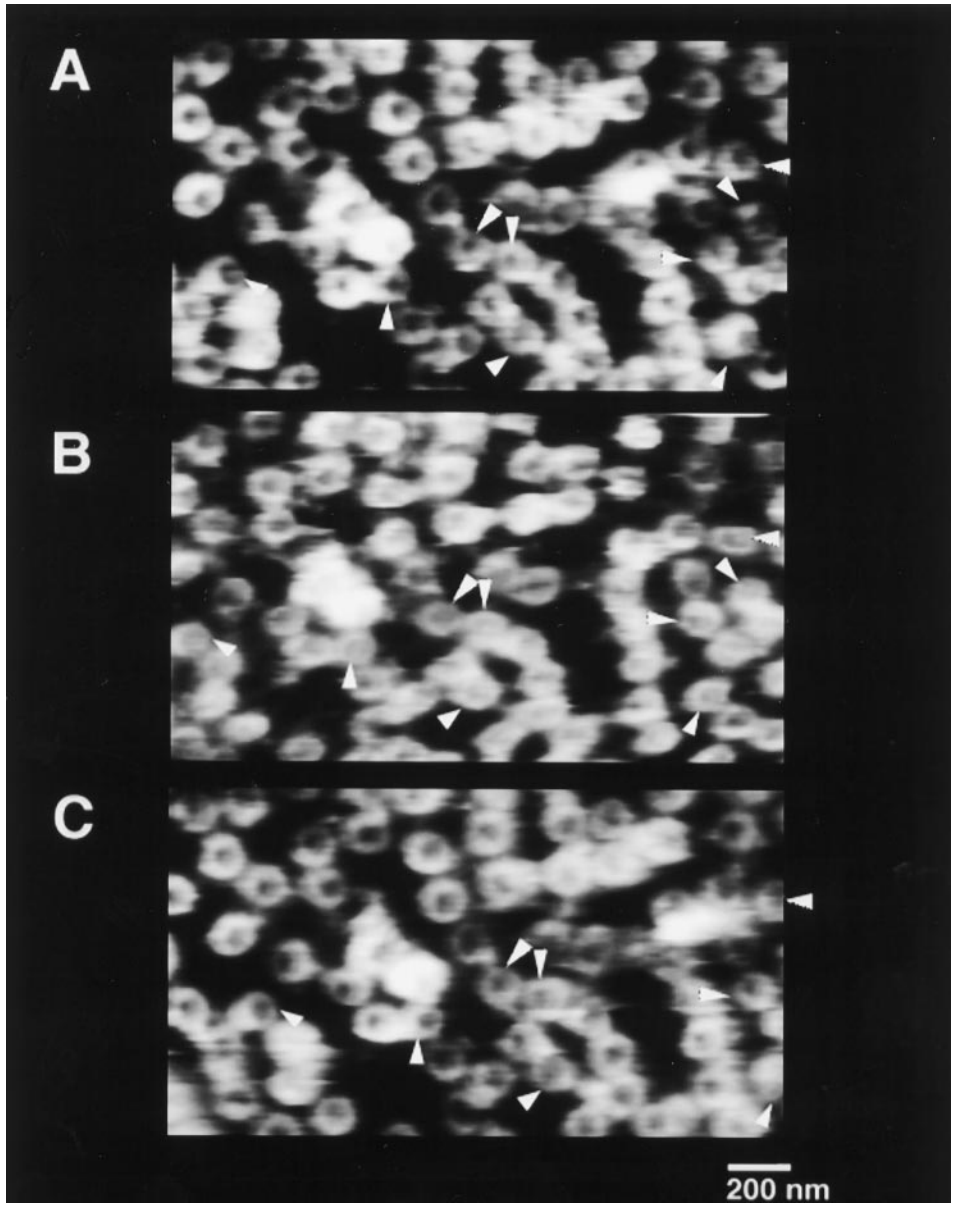

FIGURE 5 Continuous AFM imaging of NPCs in solution. Conformational change (and percent of NPCs containing the central granule) when the nuclear envelope was incubated in (*A*) normal, 200 nM Ca^{2+} (16% of 126 NPCs); (*B*) 1 μM Ins(1,4,5)P_3 (66% 0f 131 NPCs; and (*C*) 1 mM ATP plus 500 nM [Ca^{2+}] (27% of 117 NPCs). Approximately 10 min elapsed between each image. Slight shifting of the frame occurs due to movement during the solution change. Conformational changes are seen most clearly in the NPCs indicated by arrows.

cells, isolated nuclei, and nuclear ghosts (Stehno-Bittel et al., 1995b). The molecules blocked by depletion included dextran-bound dyes with intermediate molecular weights (~10 kDa) but not very low molecular weight compounds such as Lucifer Yellow (500 Da) and ions such as Mn^{2+} or Ca^{2+}.

A Ca^{2+} depletion sensor in the nuclear cisterna has not been identified. However, gp210, a Ca^{2+}-binding glycoprotein, may form part of the NPC lumenal domain (Greber et al., 1990) since a monoclonal antibody directed to a lumenal epitope of gp210 reduced the passive diffusion of proteins (Greber and Gerace, 1992). This, or other related molecules, could trigger rearrangement within the lumenal domain and result in a conformational change in the inner spoke ring and central granule (Perez-Terzic et al., 1997).

To return to the three hypotheses for the role of the central granule, we can rule out the possibility that the central granule is a simple fixation artifact since the NPCs studied here were not dried or fixed. We cannot rule out the possibility that the collapsed nuclear basket is the nuclear granule because we cannot image both sides of the NPC at once. If it is the nuclear basket, it appears to occupy one of only two collapsed positions. Similarly, it seems unlikely that the central granule represents trapped cargo, since the material, no matter what its nature, would be trapped in only one of two positions to explain our observations. Despite the fact that the NPC conformational change occurs under ionic conditions similar to the cytoplasm of intact cells, it is not possible to image the NPC in an intact cell. Thus the idea that the central granule is the NPC gate translocated upon store depletion remains a hypothesis. However, nuclear transport does activate and inactivate during the cell cycle, with A and B type cyclins moving into the nucleus during the S and M phase (Pines and Hunter, 1991), and protein

phosphatase 1 moving into the nucleus during the G2 phase of the cell cycle (Inagaki et al., 1994). Passive diffusion across the nuclear envelope decreases at 2–3 h after the onset of anaphase (Feldherr and Akin, 1990), correlating with a decrease in nuclear phosphatidylinositols observed after release from the G1/S boundary of the cell cycle (York and Majerus, 1994). Also, growth factors modulate the production of IP_3 and induce changes in passive diffusion across nuclei (Jiang and Schindler, 1988). These results indicate that the NPC can be regulated in response to different growth states of a cell and that the permeability of the NPC may vary during different stages of cellular activity.

REFERENCES

Allen, T. D., S. A. Rutherford, G. R. Bennion, C. Wiese, S. Riepert, E. Kiseleva, and M. W. Goldberg. 1998. Three-dimensional surface structure analysis of the nucleus. *Methods Cell Biol.* 53:125–138.

Akey, C. W. 1990. Visualization of transport-related configurations of the nuclear pore transporter. *Biophys. J.* 58:341–355.

Akey, C. W., and M. Radermacher. 1993. Architecture of the Xenopus nuclear pore complex revealed by three-dimensional cryo-electron microscopy. *J. Cell Biol*. 122:1–19.

Feldherr, C. M., and D. Akin. 1990. The permeability of the nuclear envelope in dividing and nondividing cell cultures. *J. Cell Biol.* 111:1–8.

Folprecht, G., S. Schneider, and H. Oberleithner. 1996. Aldosterone activates the nuclear pore transporter in cultured kidney cells imaged with atomic force microscopy. *Pfluegers Arch.* 432:831–838.

Forbes, D. J. 1992. Structure and function of the nuclear pore. *Annu. Rev. Cell Biol.* 8:495–527.

Gerace, L., and B. Burke. 1988. Functional organization of the nuclear envelope. *Annu. Rev. Cell Biol.* 4:335–374.

Goldberg, M. W., and T. D. Allen. 1995. Structural and functional organization of the nuclear envelope. *Curr. Opin. Cell Biol.* 7:301–309.

Greber, U. F., and L. Gerace. 1992. Nuclear import protein is inhibited by an antibody to a lumenal epitope of a nuclear pore complex glycoprotein. *J. Cell. Biol*. 116:15–30.

Greber, U. F., and L. Gerace. 1995. Depletion of calcium from the lumen of endoplasmic reticulum reversible inhibits passive diffusion and signal-mediated transport into the nucleus. *J. Cell. Biol.* 128:5–25.

Greber, U. F., A. Senior, and L. Gerace. 1990. A major glycoprotein of the nuclear pore complex is a membrane-spanning polypeptide with a large lumenal domain and a small cytoplasmic tail. *EMBO J.* 9:1495–1502.

Greber, U. F., M. Suomalainen, R. P. Stidwill, K. Boucke, M. W. Ebersold, and A. Helenius. 1997. The role of the nuclear pore complex in adenovirus DNA entry. *EMBO J.* 16:5998–6007.

Hanover, J. A. 1992. The nuclear pore: at the crossroads. *FASEB J.* 6:2288–2295.

Hinshaw, J. E., B. O. Carragher, and R. A. Milligan. 1992. Architecture and design of the nuclear pore complex. *Cell*. 69:1133–1141.

Jarnik, M., and U. Aebi. 1991. Toward a more complete 3-D structure of the nuclear pore complex. *J. Struct. Biol.* 107:291–308.

Jiang, L. W., and M. Schindler. 1988. Nuclear transport in 3T3 fibroblasts: effects of growth factors, transformation, and cell shape. *J. Cell Biol.* 106:13–19.

Inagaki, N., M. Ito, T. Nakano, and M. Inagaki. 1994. Spatiotemporal distribution of protein kinase and phosphatase activities. *Trends Biochem. Sci.* 19:448–452.

Lechleiter, J., and D. E. Clapham. 1992. Molecular mechanisms of intracellular calcium release in *Xenopus laevis* oocytes. *Cell*. 69:1–20.

Mak, D. O., and J. K. Foskett. 1994. Single-channel inositol 1,4,5-trisphosphate receptor currents revealed by patch clamp of isolated Xenopus oocyte nuclei. *J. Biol. Chem*. 269:29375–29378.

Mattaj, I. W., and L. Englmeier. 1998. Nucleocytoplasmic transport—the soluble phase. *Annu. Rev. Biochem.* 67:265–306.

Pante, N., and U. Aebi. 1994. Toward the molecular details of the nuclear pore complex at the molecular level. *J. Struct. Biol*. 3:178–189.

Perez-Terzic, C. M., M. Jaconi, and D. E Clapham. 1997. Nuclear calcium and the regulation of the nuclear pore complex. *Bioessays*. 19:787–792.

Perez-Terzic, C., J. Pyle, M. Jaconi, L. Stehno-Bittel, and D. E. Clapham. 1996. Conformational states of the nuclear pore complex induced by depletion of nuclear calcium stores. *Science*. 273:1875–1877.

Pines, J., and T. Hunter. 1991. Human cyclins A and B1 are differentially located in the cell and undergo cell cycle-dependent nuclear transport. *J. Cell Biol*. 115:1–17.

Rakowska, A., T. Danker, S. W. Schneider, and H. Oberleithner. 1998. ATP-induced shape change of nuclear pores visualized with the atomic force microscope. *J. Membr. Biol.* 163:129–136.

Stehno-Bittel, L., A. Lückhoff, and D. E. Clapham. 1995a. Calcium release from the nucleus by $InsP_3$ receptor channels. *Neuron*. 14:163–167.

Stehno-Bittel, L., C. Perez-Terzic, and D. E. Clapham. 1995b. Diffusion across the nuclear envelope inhibited by depletion of the nuclear Ca^{2+} store. *Science*. 270:1835–1838.

Strübing, C., and D. E. Clapham. 1999. Active nuclear import, and export is independent of lumenal Ca^{2+} stores in intact mammalian cells. *J. Gen. Physiol.* 113:239–248.

York, J. D., and P. W. Majerus. 1994. Nuclear phosphatidylinositols decrease during S-phase of the cell cycle in HeLa cells. *J. Biol. Chem*. 269:7847–7850.